VIP Supramolecular Chemistry Very Important Paper

Deutsche Ausgabe: DOI: 10.1002/ange.201503614
Internationale Ausgabe: DOI: 10.1002/anie.201503614

Photocontrolled Reversible Conversion of Nanotube and Nanoparticle Mediated by β-Cyclodextrin Dimers**

*He-Lue Sun, Yong Chen, Jin Zhao, and Yu Liu**

Abstract: *A photochemically interconvertible supramolecular nanotube–nanoparticle system was constructed through secondary assembling of self-aggregates of amphiphilic porphyrin derivatives mediated by trans- and cis-azobenzene-bridged bis(permethyl-β-cyclodextrin). Significantly, these nanotubes and nanoparticles were able to interconvert upon irradiation at different wavelengths, and this photocontrolled morphological conversion is reversible and recyclable for tens of times, which will provide a feasible and convenient way to construct the ordered nanostructure with various morphologies that can be smartly controlled by the environmentally benign external stimulus.*

Controllable supramolecular nanoassembly has attracted increasing attention due to its wide application in the fields of catalysis,[1] nanoscience,[2] and drug delivery.[3] Supramolecular assembling is an effective approach for the construction of controllable nanoscaled assemblies[4] that are responsive to various external stimuli, such as temperature, pH, redox conditions, enzymes, and light. Among these external stimuli, light is of particular interest because of its noninvasive, clean and remote-controlling properties.[5] In the last decade, a number of photocontrolled supramolecular assemblies, including photoswitchable supramolecular hydrogel,[6] photoresponsive artificial muscle,[7] photodriven pseudorotaxane,[8] photocontrolled supramolecular assembly,[9] have been successfully constructed using azobenzene and cyclodextrin (CD) components, where the reversible photoisomerization of the former and/or the different binding behaviors of *trans*- and *cis*-azobenzenes with CD play major roles.[10] However, these studies have focused mainly on the photocontrolled assembly/disassembly process, while the morphological conversion of supramolecular assembly switched by light irradiation has rarely been reported. Kim and co-workers[11] reported a one-cycle morphological conversion of pyrene-modified dendritic self-assembly induced by the sequential addition of CD and poly(propylene glycol). Herein, we report a photocontrolled reversible and repeatable nanotube–nanoparticle morphological conversion of the secondary assembly of amphiphilic porphyrin (**G**) mediated by azobenzene-bridged bis(permethyl-β-CD) (**H**; Scheme 1).

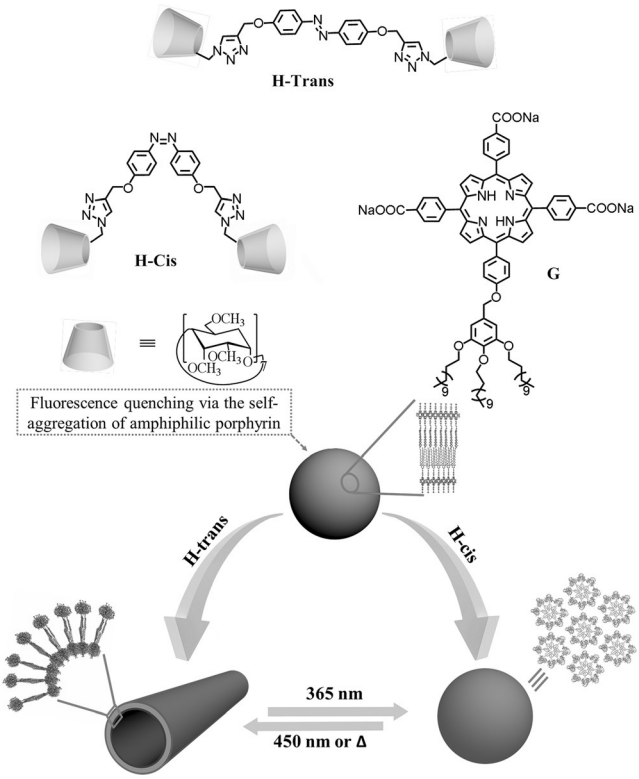

Scheme 1. Schematic presentation of **H**, **G**, and secondary assembly.

The self-assembly behavior of amphiphilic guest **G** was investigated by UV/Vis and fluorescence spectroscopy, dynamic light scattering (DLS) and transmission electron microscopy (TEM). As shown in Figure S6 (see the Supporting Information), UV/Vis and fluorescence spectra of **G** differed significantly in aqueous buffer solution and in methanol solution. In methanol, the UV/Vis spectrum of **G** showed a sharp peak at 417 nm, which is assigned to the Soret band of the porphyrin moiety. However, in aqueous buffer, this peak obviously broadened with accompanying blue-shift to give a profile very similar in shape to the one reported for porphyrin H-aggregates.[12] In addition, guest **G** emitted strong fluorescence in methanol but barely fluoresced in aqueous buffer. Therefore, we concluded that guest **G** formed H-type self-aggregates in aqueous solution, where the close

[*] H.-L. Sun, Dr. Y. Chen, J. Zhao, Prof. Dr. Y. Liu
Department Department of Chemistry
State Key Laboratory of Elemento-Organic Chemistry
Nankai University, Tianjin 300071 (P.R. China)
E-mail: yuliu@nankai.edu.cn
Dr. Y. Chen, Prof. Dr. Y. Liu
Collaborative Innovation Center of Chemical Science and Engineering
Nankai University, Tianjin 300071 (P.R. China)

[**] We thank 973 Program (grant number 2011CB932502) and NSFC (grant numbers 91227107, 21432004, and 21272125) for financial support.

Supporting information for this article is available on the WWW under http://dx.doi.org/10.1002/anie.201503614.

proximity of porphyrin moieties within aggregate leads to the self-quenching of fluorescence. Indeed, the addition of methanol disassembled the H-type self-aggregate, leading to the enhanced fluorescence assignable to porphyrin monomer.

The morphological information of the self-aggregates came from DLS and TEM. The DLS data show that guest **G** form large aggregates with an average hydrodynamic diameter of about 180 nm, while the TEM images revealed a number of spherical nanostructures with an average diameter of 150 nm, which is slightly smaller than that estimated from the DLS measurements, probably due to the shrinking of nanoparticles in the drying stage of the TEM sample preparation.[13] The assembly mechanism of **G** may be similar to the one reported previously.[12a] Therein, the hydrophilic porphyrin moieties are located in the outer layer, while the hydrophobic tails gather together to form the hydrophobic inner layer, and the π-π and hydrophobic interactions jointly stabilize the self-aggregate. The critical aggregation concentration (CAC) of **G** was determined as about 42.5 nM by concentration-dependent fluorescence spectroscopy (Figure S8).

After validating the formation of self-aggregates, we investigated the secondary assembly of **G** mediated by bis(permethyl-β-CD) **H**. There are two inherent advantages of choosing **H** for mediating the secondary assembly of **G**. 1) Permethyl-β-CD can very strongly bind water-soluble porphyrin in aqueous solution.[14] In control experiments (Figures S10 and S11), the complexation stoichiometry between monomeric permethyl-β-CD and guest **G** was determined as 2:1 by Job analysis and the binding constants as $K_1 = 3.4 \times 10^8\,M^{-1}$ and $K_2 = 1.2 \times 10^7\,M^{-1}$ by UV/Vis titration. This strong binding will enable the spontaneous secondary assembling upon mixing **G** and **H** in aqueous solution. (2) The photoisomerization of azobenzene bridge induces the shape-change of **H** and thus leads to the topological transformation of secondary assembly. As shown in Figure 1b, upon addition of **H**, the broadened Soret band of **G** assignable to the H-type self-aggregate became sharper with accompanying red-shift from 404 to 417 nm, and the fluorescence intensity of **G** was enhanced by a factor of about 30 (Figure S12a). The resulting UV/Vis and fluorescence spectra of **H/G** system are very similar to those of free **G** in methanol. Moreover, the **H/G** system exhibited a stronger Cotton effect in circular dichroism spectrum than free **G** (Figure 1a). These phenomena jointly indicate that the association of **H** with **G** disrupts the self-aggregate of **G** and produces the supramolecular **H/G** assembly. The Job analysis of the UV/Vis spectral data (Figure S13 and S15) gave the stoichiometric 1:1 binding radio between **H** and **G**, and the apparent binding constant was calculated as $2.37 \times 10^6\,M^{-1}$ and $8.45 \times 10^6\,M^{-1}$ for the association of **G** with *trans*- and *cis*-isomer of **H**, respectively, from the UV/Vis spectral titration data (Figures S14 and S16).

Interestingly, the **H/G** supramolecular conjugate exhibited different assembling behavior from free **G**. Generally, the azobenzene bridge exists in its *trans*-form. DLS data (Figure 2a) showed that the assembly of **G** with the *trans*-isomer of **H** (**H-trans**) possesses an average hydrodynamic diameter of up to thousands of nanometers, which is dramatically larger than that observed for **G** aggregate (ca. 180 nm). Direct

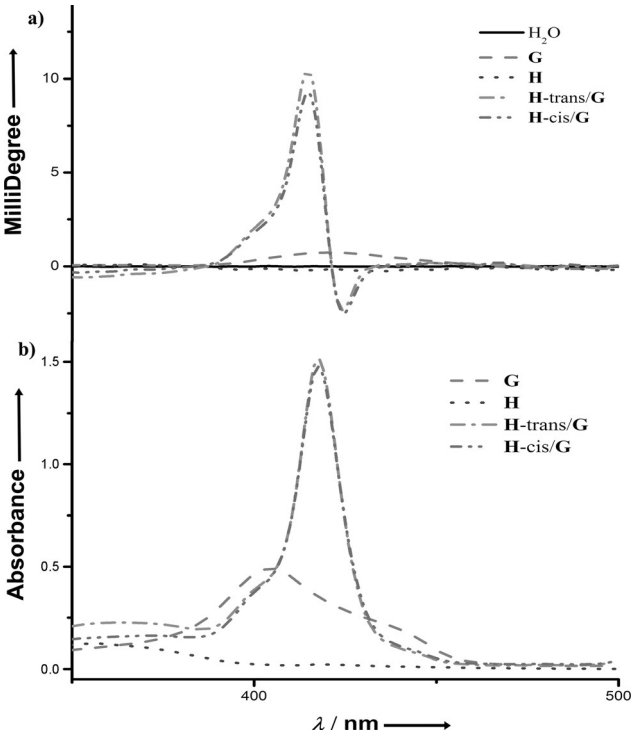

Figure 1. a) Circular dichroism spectra, b) UV/Vis spectra of **G**, **H**, **H-trans/G**, and **H-cis/G** in phosphate buffer (pH 7.2, 0.1 M) at 25 °C. ([**G**] = [**H**] = 5 μM).

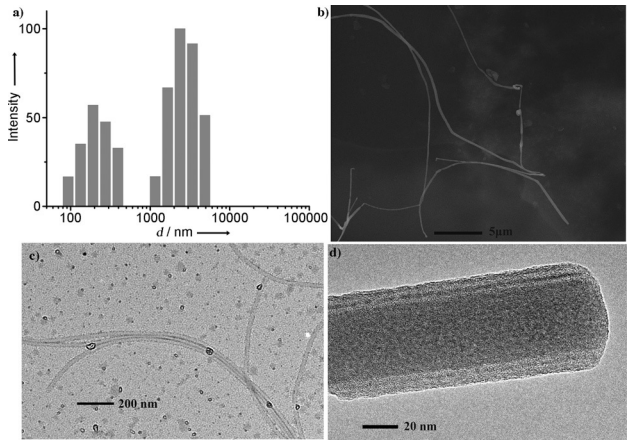

Figure 2. a) DLS, b) SEM (scale bar = 5 μm), c) TEM (scale bar = 200 nm), and d) enlarged TEM (scale bar = 20 nm) images of nanotubes formed from **H-trans** and **G** ([**H**] = [**G**] = 5 μM; pH 7.2).

morphological information of the **H-trans/G** nanoarchitecture was provided by SEM and TEM observations. As shown in Figure 2b and S16a, SEM images of an air-dried equimolar solution of **H-trans** and **G** exclusively displayed a number of open-ended, curved tubular structures with large aspect ratios, and the length reaches tens of micrometer. Moreover, TEM images clearly showed the hollow tubular structure of a uniform hollow size (Figure 2c and d). On the basis of the TEM analysis, the average inner and outer diameters of the **H-trans/G** nanotubes are about 45 and 61 nm, respectively,

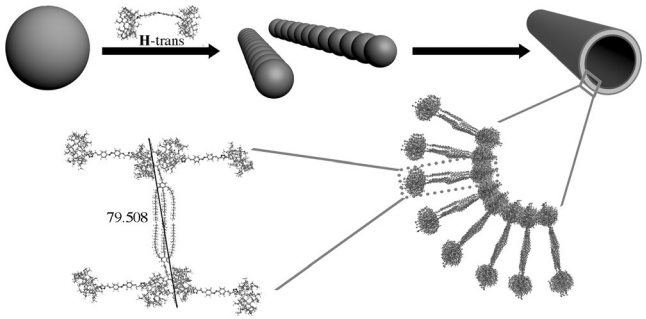

Figure 3. Schematic presentation of the secondary assembly of **G** mediated by **H-trans**.

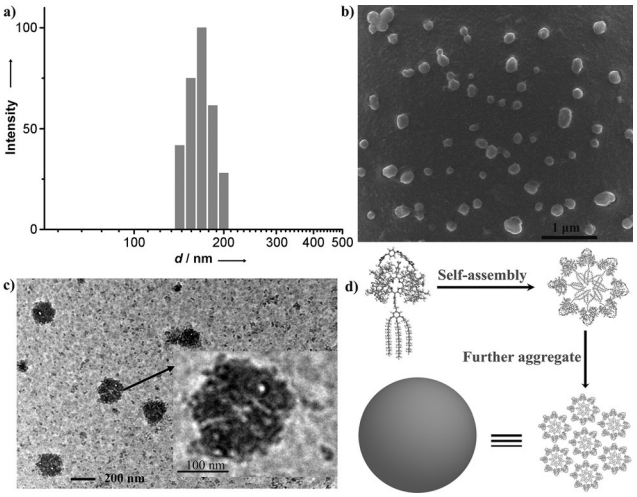

Figure 4. a) DLS, b) SEM (scale bar = 1 μm), and c) TEM images of **H/G** assembly after light (365 nm) irradiation for 20 minutes (scale bar = 200 nm; inset: scale bar = 100 nm). ([**H**] = [**G**] = 5 μM, pH 7.2).

with a wall thickness of about 8 nm. Based on a computer simulation study, the calculated wall thickness of nanotubes was 7.9 nm, which nicely agrees with the value (ca. 8 nm) determined from the TEM image (Figure 3). Interestingly, the concentration-dependent TEM images revealed that, at a relatively low concentration, a number of rod-like structures were observed. Each rod-like structure was composed of a number of spherical nanoparticles, the size of which was very similar to that of the self-aggregate of **G** (Figure S17). At higher concentrations of **H-trans/G**, these rod-like structures turned to nanotubes. Combining these observations, we can reasonably deduce that the **H-trans**-mediated secondary assembly of **G** is responsible for the formation of nanotubes, and that the interior and exterior surfaces of nanotubes are composed of the highly stable **H-trans**/porphyrin-associated units, whereas the hydrophobic alkyl chains of **G** interlace with each other in the middle of the tubular walls, as illustrated in Figure 3.

Significantly, after irradiation of the solution of **H-trans/G** at 365 nm for 20 minutes, the original diameter of **H-trans/G** (thousands of nanometers, measured by DLS) was greatly reduced to 180 nm (measured by DLS), as shown in Figure 4a. In addition, visible information of the photoinduced morphological conversion was obtained from the SEM and TEM images (Figure 4b and c). Therein, the long **H-trans/G** nanotubes turned to a number of solid nanoparticles with an average diameter of 180–200 nm. These nanoparticles were appreciably larger and denser than those formed by the self-aggregation of **G**. Job analysis gave the complexation stoichiometry between the *cis*-isomer of **H** (**H-cis**) and **G** as 1:1. Moreover, the binding constant of **H-cis** with **G** ($8.45 \times 10^6\ M^{-1}$) was appreciably higher than that of **H-trans** probably because of the cooperative binding of two β-CD cavities in **H-cis** with a **G** molecule. Based on this information, we deduce that the morphological conversion is driven by the photoinduced geometrical change of **H** from the *trans*-isomer (**H-trans**) to *cis*-isomer (**H-cis**). That is, under the light irradiation, the **H-trans** units in **H-trans/G** secondary assembly convert to **H-cis**, and these **H-cis** units subsequently interact with **G** through sandwich complexation. The resulting **H-cis/G** sandwich complexes, possessing a larger hydrophilic head than free **G**, first self-assemble to small micelles (computational structure in Figure 4d). Then, these micelles further aggregate to form larger nanoparticles (Figure 4d), most probably by the small micelle aggregation mechanism or the multicompartment micelle formation mechanism.[13] In a control experiment, an equimolar mixture of **H-cis** and **G** gave the DLS and TEM results similar to those shown in Figure 4. Upon irradiation at 365 nm, the **H-trans/G** assembly exhibited moderate fluorescence assignable to the emission of porphyrin. This means that, in addition to the isomerization to the cis-isomer, the excited *trans*-azobenzene transfers the excitation energy at least in part to a nearby porphyrin, leading to the porphyrin fluorescence.

It is also important to investigate the repetitiveness of the photodriven morphology conversion. As shown in Figure 5, the absorbance of **H-trans** at 357 nm, assigned to the characteristic absorption of the π-π* transition of *trans*-azobenzene, dramatically decreased under the light irradiation at 365 nm, indicating photoisomerization of the azobenzene moiety from *trans* to *cis*.[10a,15] However, the decreased intensity at 357 nm was recovered to its original level upon subsequent irradiation at 450 nm because of the reverse photoisomerization from *cis* to *trans*. In addition, the fluorescence excitation spectrum of **H-cis/G** at 450 nm was very weak, and **H-cis/G** barely fluoresced upon excitation at 450 nm. This indicates that the irradiation at 450 nm predominantly excites the *cis*-azobenzene chromophore, although the direct excitation of porphyrin cannot be rigorously ruled out. Significantly, this cycle can be repeated tens of times. In addition, TEM and DLS experiments confirmed that the assembly morphology can be switched between nanotube and nanoparticle by irradiating at different wavelengths (Figures S18 and S19). These phenomena jointly indicate the good reversibility and repetitiveness of the photocontrolled nanotube–nanoparticle morphological conversion.

In summary, taking advantage of the strong binding affinity between permethyl-β-CD and water-soluble tetraarylporphyrins as well as the photoisomerization property of azobenzene derivatives, an azobenzene-bridged bis(permethyl-β-CD) was successfully applied to the construction of the secondary assembly of amphiphilic porphyrin deriva-

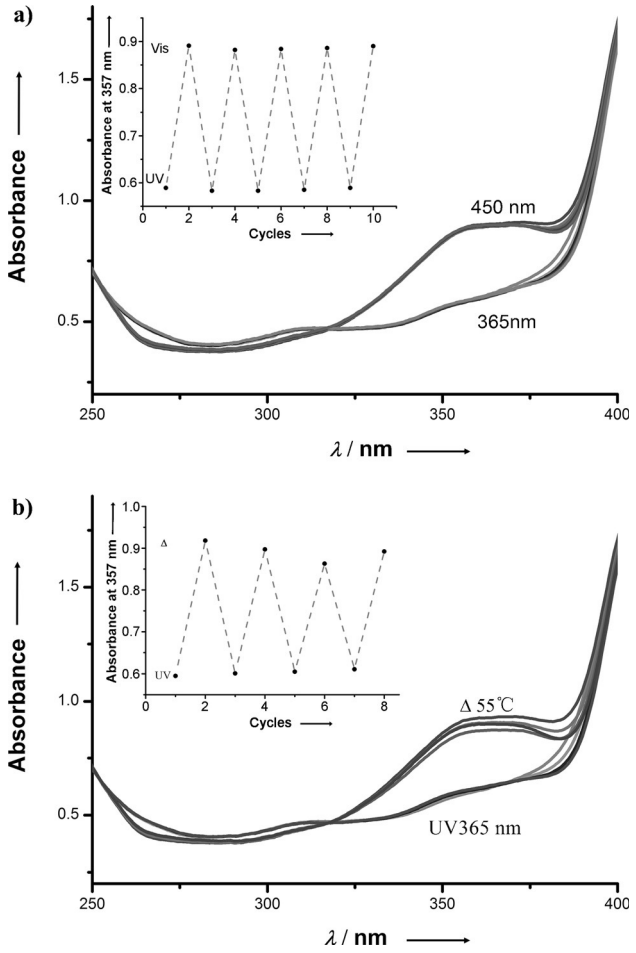

Figure 5. UV/Vis spectra of **H/G** assembly and (inset) absorption changes at 357 nm. a) Under light irradiation at 365 nm and 450 nm, b) under irradiation at 365 nm and heat at 55 °C. ([**H**] = [**G**] = 20 μM, pH 7.2).

tive. Crucially, the morphology of the secondary assembly can be reversibly switched between nanotube and nanoparticle under light irradiation. The photoswitchable morphological conversion property, along with the facile preparation, will make this supramolecular assembly approach well-suitable for a variety of important biomedical and material applications.

Experimental Section

Synthesis of azobenzene-bridged bis(permethyl-β-CD): 4,4′-Dipropargyloxyazobenzene[16] (0.2 mmol, 58 mg) was added to a stirred solution of 6-deoxy-6-azide-permethyl-β-CD[17] (720 mg, 0.5 mmol) in DMF (dimethylformamide; 50 mL), to which CuI (0.5 mmol, 95 mg) was added under argon at room temperature. The mixture was stirred overnight at 75 °C. After cooling to room temperature, the mixture was filtered to remove any insoluble copper salt, and the filtrate was evaporated under reduced pressure to remove excess DMF. The residue was purified by silica gel column chromatography using chloroform–methanol solution (v/v = 50:1) as elutent to give azobenzene-bridged bis(permethyl-β-CD) (71 %) as orange foam (yield 71 %). ^{1}H NMR (400 MHz, $CDCl_3$): δ = 7.87 (d, J = 8.9 Hz, 4H), 7.78 (s, 2H), 7.08 (d, J = 9.0 Hz, 4H), 5.27 (s, 4H), 5.14 (m, 12H), 5.02 (d, J = 12.7 Hz, 2H), 4.73 (m, 2H), 4.18–3.01 ppm (m, 202H). ^{13}C NMR (100 MHz, $CDCl_3$): δ = 160.2, 147.3, 143.0, 125.1, 124.4, 114.8, 99.2, 98.8, 98.3, 83.0, 82.0, 81.9, 81.8, 81.1, 80.3, 80.2, 79.9, 79.3, 71.28, 71.0, 70.8, 70.7, 70.3, 62.2, 61.8, 61.4, 61.3, 59.2, 59.1, 59.0, 58.9, 58.7, 58.6, 58.5, 58.4, 51.5 ppm. MALDI-TOF-HRMS: 3192.4603 $[M+Na]^+$, 3208.4280 $[M+K]^+$.

Keywords: conversion · photochemistry · photocontrol · self-assembly · supramolecular chemistry

How to cite: *Angew. Chem. Int. Ed.* **2015**, *54*, 9376–9380
Angew. Chem. **2015**, *127*, 9508–9512

[1] a) J. D. Crowley, K. D. Hänni, D. A. Leigh, A. M. Z. Slawin, *J. Am. Chem. Soc.* **2010**, *132*, 5309–5314; b) L. Zhu, H. Yan, C. Y. Ang, K. T. Nguyen, M. Li, Y. Zhao, *Chem. Eur. J.* **2012**, *18*, 13979–13983.
[2] a) A. Coskun, M. Banaszak, R. D. Astumian, J. F. Stoddart, B. A. Grzybowski, *Chem. Soc. Rev.* **2012**, *41*, 19–30; b) C. J. Bruns, M. Frasconi, J. Iehl, K. J. Hartlieb, S. T. Schneebeli, C. Cheng, S. I. Stupp, J. F. Stoddart, *J. Am. Chem. Soc.* **2014**, *136*, 4714–4723.
[3] a) Q.-D. Hu, G.-P. Tang, P. K. Chu, *Acc. Chem. Res.* **2014**, *47*, 2017–2025; b) D.-S. Guo, K. Wang, Y.-X. Wang, Y. Liu, *J. Am. Chem. Soc.* **2012**, *134*, 10244–10250.
[4] a) K. Kinbara, T. Aida, *Chem. Rev.* **2005**, *105*, 1377–1400; b) Y. Chen, Y. Liu, *Chem. Soc. Rev.* **2010**, *39*, 495–505; c) J.-M. Lehn, *Science* **2002**, *295*, 2400–2403.
[5] a) Y. Inoue, P. Kuad, Y. Okumura, Y. Takashima, H. Yamaguchi, A. Harada, *J. Am. Chem. Soc.* **2007**, *129*, 6396–6397; b) H.-B. Cheng, H.-Y. Zhang, Y. Liu, *J. Am. Chem. Soc.* **2013**, *135*, 10190–10193; c) Y.-X. Wang, Y.-M. Zhang, Y. Liu, *J. Am. Chem. Soc.* **2015**, *137*, 4543–4549.
[6] a) X. Liao, G. Chen, X. Liu, W. Chen, F. Chen, M. Jiang, *Angew. Chem. Int. Ed.* **2010**, *49*, 4409–4413; *Angew. Chem.* **2010**, *122*, 4511–4515; b) S. Tamesue, Y. Takashima, H. Yamaguchi, S. Shinkai, A. Harada, *Angew. Chem. Int. Ed.* **2010**, *49*, 7461–7464; *Angew. Chem.* **2010**, *122*, 7623–7626; c) H. Yamaguchi, Y. Kobayashi, R. Kobayashi, Y. Takashima, A. Hashidzume, A. Harada, *Nat. Commun.* **2012**, *3*, 603.
[7] Y. Takashima, S. Hatanaka, M. Otsubo, M. Nakahata, T. Kakuta, A. Hashidzume, H. Yamaguchi, A. Harada, *Nat. Commun.* **2012**, *3*, 1270.
[8] a) X. Ma, Q. Wang, D. Qu, Y. Xu, F. Ji, H. Tian, *Adv. Funct. Mater.* **2007**, *17*, 829–837; b) D.-H. Qu, Q.-C. Wang, J. Ren, H. Tian, *Org. Lett.* **2004**, *6*, 2085–2088; c) J. Wang, H.-Y. Zhang, X.-J. Zhang, Z.-H. Song, X.-J. Zhao, Y. Liu, *Chem. Commun.* **2015**, *51*, 7329–7332.
[9] a) Y. Wang, N. Ma, Z. Wang, X. Zhang, *Angew. Chem. Int. Ed.* **2007**, *46*, 2823–2826; *Angew. Chem.* **2007**, *119*, 2881–2884; b) J. Zou, B. Guan, X. Liao, M. Jiang, F. Tao, *Macromolecules* **2009**, *42*, 7465–7473.
[10] a) Z. Y. Li, J. H. Liang, W. Xue, G. X. Liu, S. H. Liu, J. Yin, *Supramol. Chem.* **2014**, *26*, 54–65; b) A. Harada, *Acc. Chem. Res.* **2001**, *34*, 456–464; c) Y. Liu, S. Kang, Y. Chen, Y.-W. Yang, J. Huskens, *J. Inclusion Phenom. Macrocyclic Chem.* **2006**, *56*, 197–201.
[11] C. Park, I. H. Lee, S. Lee, Y. Song, M. Rhue, C. Kim, *Proc. Natl. Acad. Sci. USA* **2006**, *103*, 1199–1203.
[12] a) S. V. Bhosale, S. V. Bhosale, G. V. Shitre, S. R. Bobe, A. Gupta, *Eur. J. Org. Chem.* **2013**, 3939–3954; b) S. Tomas, L. Milanesi, *J. Am. Chem. Soc.* **2009**, *131*, 6618–6623.
[13] P. Huang, D. Wang, Y. Su, W. Huang, Y. Zhou, D. Cui, X. Zhu, D. Yan, *J. Am. Chem. Soc.* **2014**, *136*, 11748–11756.
[14] a) K. Kano, H. Kitagishi, C. Dagallier, M. Kodera, T. Matsuo, T. Hayashi, Y. Hisaeda, S. Hirota, *Inorg. Chem.* **2006**, *45*, 4448–4460; b) K. Kano, R. Nishiyabu, T. Asada, Y. Kuroda, *J. Am. Chem. Soc.* **2002**, *124*, 9937–9944; c) Y. Liu, C.-F. Ke, H.-Y. Zhang, J. Cui, F. Ding, *J. Am. Chem. Soc.* **2007**, *129*, 600–605;

d) K. Sasaki, H. Nakagawa, X. Zhang, S. Sakurai, K. Kano, Y. Kuroda, *Chem. Commun.* **2004**, 408 – 409.
[15] a) Y. Wang, P. Han, H. Xu, Z. Wang, X. Zhang, A. V. Kabanov, *Langmuir* **2009**, *25*, 709 – 715; b) A. A. Beharry, G. A. Woolley, *Chem. Soc. Rev.* **2011**, *40*, 4422 – 4437.
[16] P. Vanoppen, P. C. M. Grim, M. Rücker, S. De Feyter, G. Moessner, S. Valiyaveettil, K. Müllen, F. C. De Schryver, *J. Phys. Chem.* **1996**, *100*, 19636 – 19641.
[17] a) C. Hocquelet, J. Blu, C. K. Jankowski, S. Arseneau, D. Buisson, L. Mauclaire, *Tetrahedron* **2006**, *62*, 11963 – 11971; b) M. T. Reetz, S. R. Waldvogel, *Angew. Chem. Int. Ed. Engl.* **1997**, *36*, 865 – 867; *Angew. Chem.* **1997**, *109*, 870 – 873.

Received: April 20, 2015
Revised: May 18, 2015
Published online: June 18, 2015

